

Supplementary Information

Cu(II) nanocluster-grafted, Nb-doped TiO₂ as an efficient visible-light-sensitive photocatalysts based on energy-level matching between surface and bulk states

Min Liu,[‡] Xiaoqing Qiu,[‡] Kazuhito Hashimoto^{*,‡,§} and Masahiro Miyauchi,^{*,†,||}

[†]Department of Metallurgy and Ceramics Science, Graduate School of Science and Engineering, Tokyo Institute of Technology, 2-12-1 Ookayama, Meguro-ku, Tokyo 152-8552, Japan.

[‡]Research Center for Advanced Science and Technology, The University of Tokyo, 4-6-1 Komaba, Meguro-ku, Tokyo 153-8904, Japan.

[§]Graduate School of Engineering, The University of Tokyo, 7-3-1 Hongo, Bunkyo-ku, Tokyo 113-8656, Japan.

^{||}Japan Science and Technology Agency (JST), ACT-C, 4-1-8 Honcho Kawaguchi, Saitama 332-0012, Japan.

Email: mmiyauchi@ceram.titech.ac.jp, hashimoto@light.t.u-tokyo.ac.jp

Contents

Table S1, S2

Figs. S1 to S16

Reference

Table S1. ICP measurement of Cu(II)-Nb_xTi_{1-x}O₂.

sample	Cu(II)-Nb_xTi_{1-x}O₂				
Initial Nb (wt%)	0.01	0.05	0.1	0.5	1
Measured Nb (wt%)	0.011	0.055	0.111	0.506	0.972

Table S2. BET surface area of bare TiO₂, Nb_xTi_{1-x}O₂, Cu(II)-TiO₂, and Cu(II)-Nb_xTi_{1-x}O₂.

Sample	TiO ₂	Nb _x Ti _{1-x} O ₂	Cu(II)-TiO ₂	Cu(II)-Nb _x Ti _{1-x} O ₂
BET surface area (m ² /g)	6.03	5.76	5.93	5.84

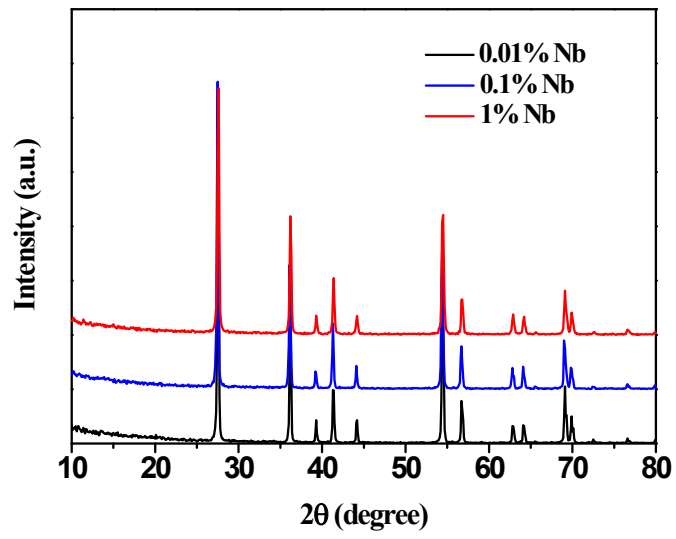


Figure S1. XRD patterns of 0.01 wt%, 0.1 wt% and 1 wt% Nb doped TiO₂.

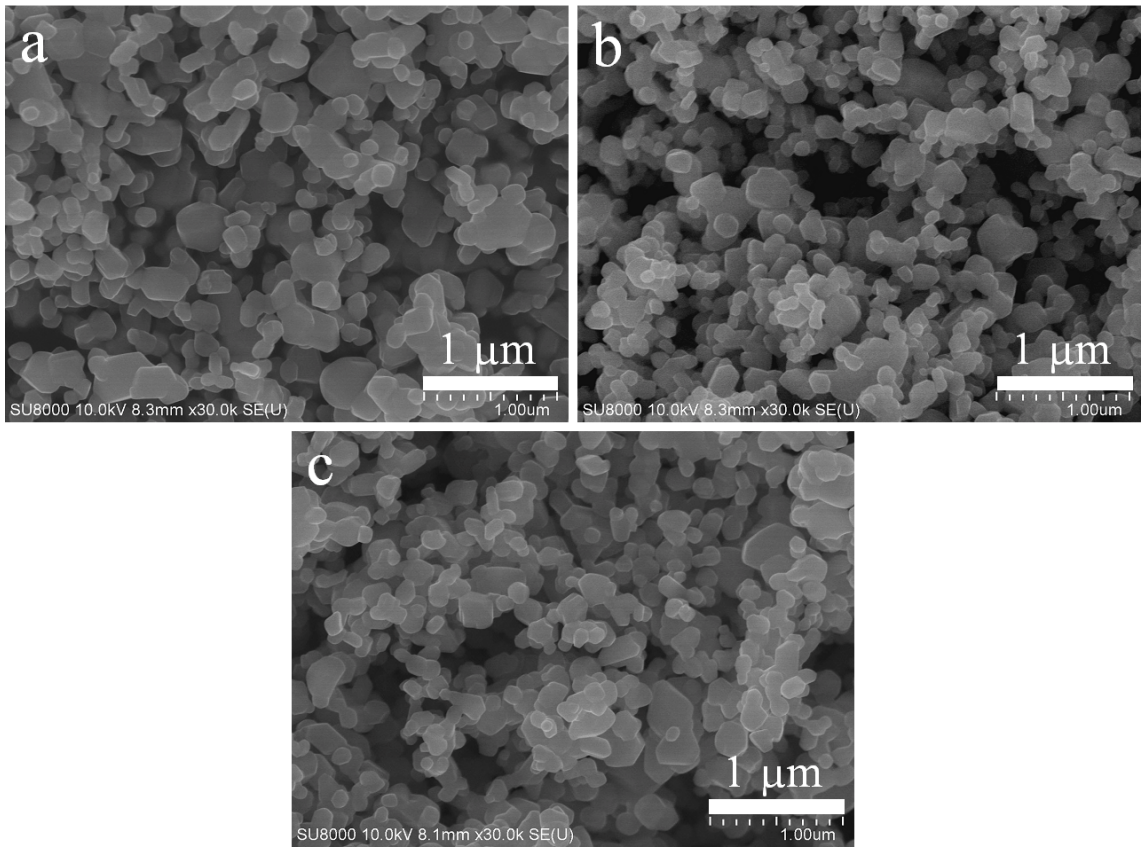


Figure S2. SEM images of $\text{Nb}_x\text{Ti}_{1-x}\text{O}_2$ at (a) $x=0.01$ wt%, (b) $x=0.1$ wt%, and (c) $x=1$ wt%, respectively.

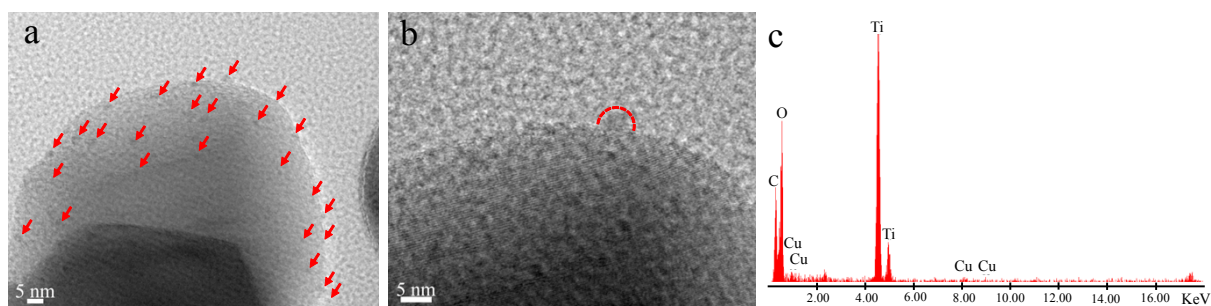


Figure S3. (a) TEM, (b) HRTEM images and (c) EDS pattern of $\text{Cu(II)-Nb}_x\text{Ti}_{1-x}\text{O}_2$. Nanoclusters (marked by red arrows) were highly dispersed on the $\text{Nb}_x\text{Ti}_{1-x}\text{O}_2$ surface. In Figure S3b, a short dashed curve is outlined the Cu(II) nanoclusters. The good attachment of nanoclusters and $\text{Nb}_x\text{Ti}_{1-x}\text{O}_2$ was clearly observed. Figure S3c shows the result of EDS point analysis on the corresponding Cu(II) nanocluster marked by the short dashed curve in Figure S3b.

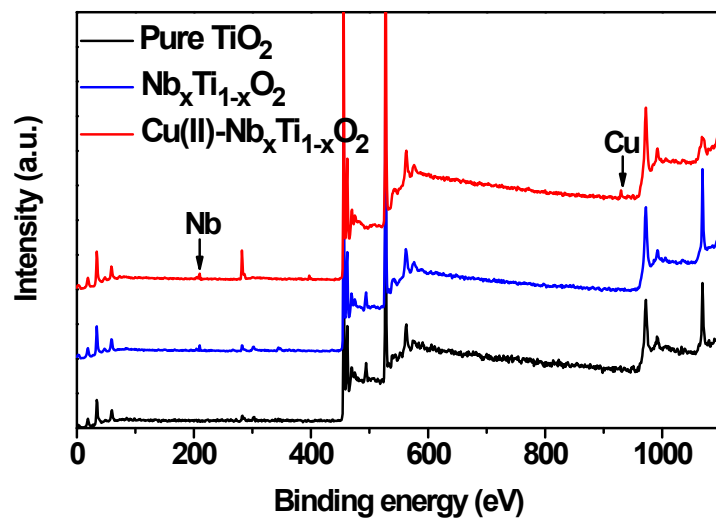


Figure S4. Full-scale XPS spectra of pure TiO₂, Nb_xTi_{1-x}O₂, and Cu(II)-Nb_xTi_{1-x}O₂, respectively.

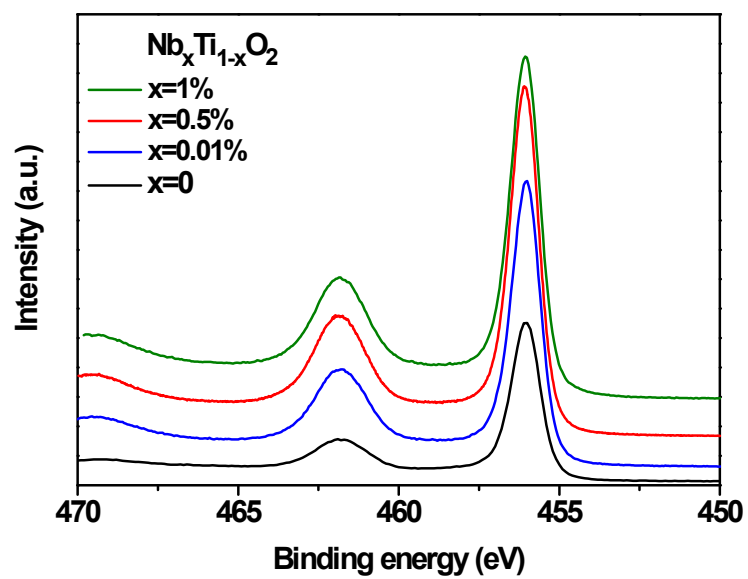


Figure S5. Ti 2p core-level spectra of pure TiO_2 , and $\text{Nb}_x\text{Ti}_{1-x}\text{O}_2$ at $x=0.01$ wt%, 0.5 wt% and 1 wt%, respectively.

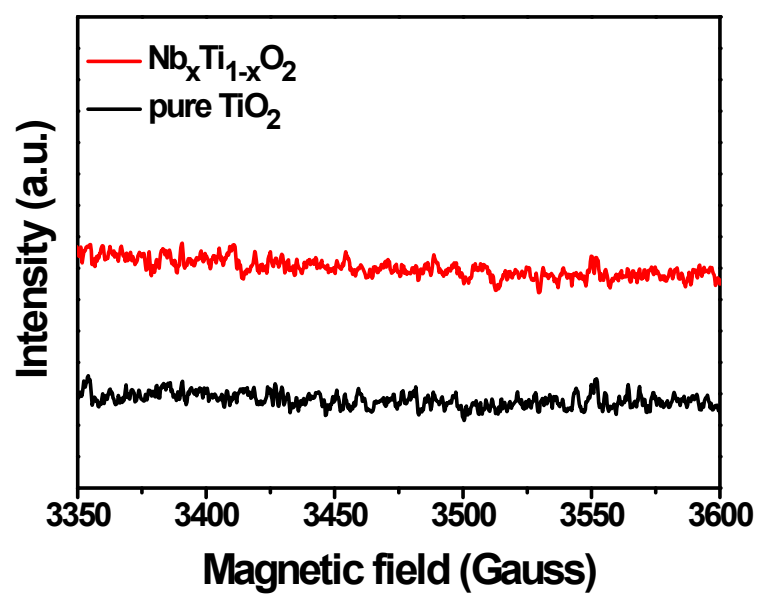


Figure S6. ESR spectra of pure TiO_2 and $\text{Nb}_x\text{Ti}_{1-x}\text{O}_2$ at 0.1 wt%.

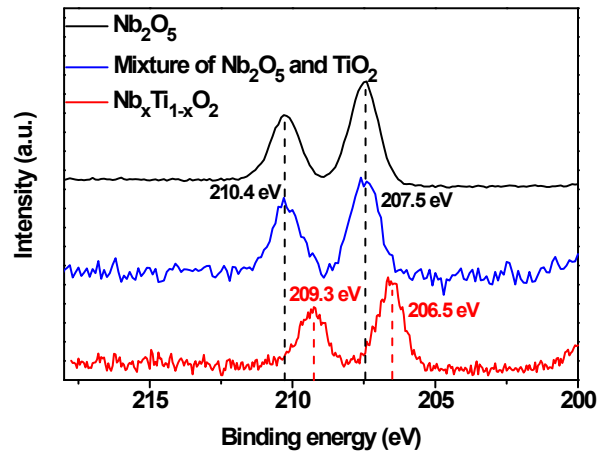


Figure S7. Nb 3d core-level spectra of pure Nb_2O_5 , physical mixed Nb_2O_5 and TiO_2 and $\text{Nb}_x\text{Ti}_{1-x}\text{O}_2$ at $x = 0.1$ wt%, respectively.

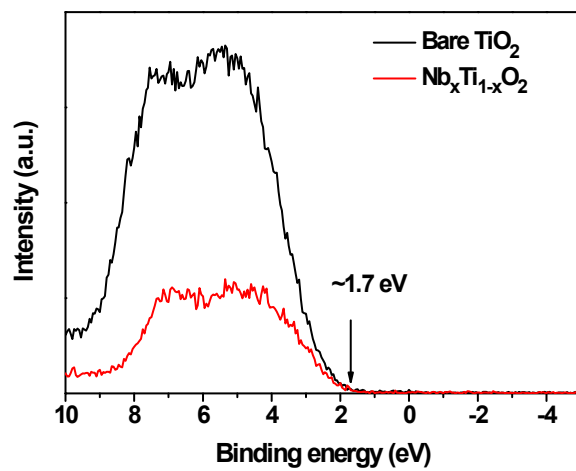


Figure S8. VB XPS of bare TiO₂, and Nb_xTi_{1-x}O₂ at x= 0.1 wt%, respectively.

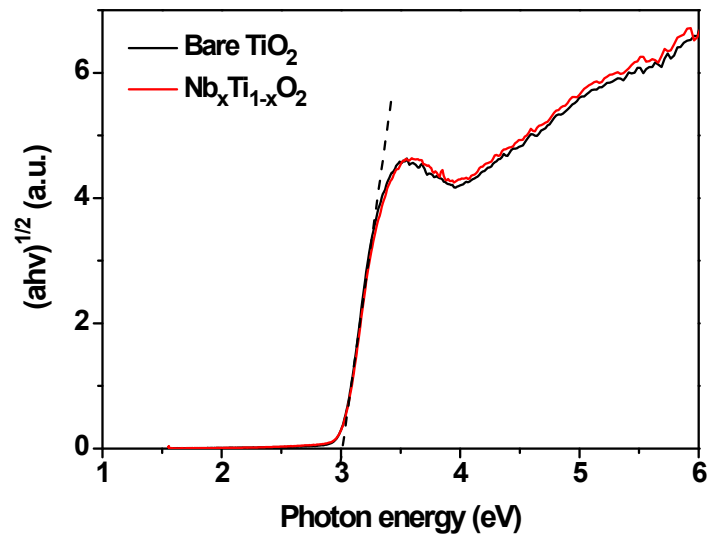


Figure S9, Band gap of bare TiO₂ and Nb_xTi_{1-x}O₂ according to the Kubelka–Munk function.

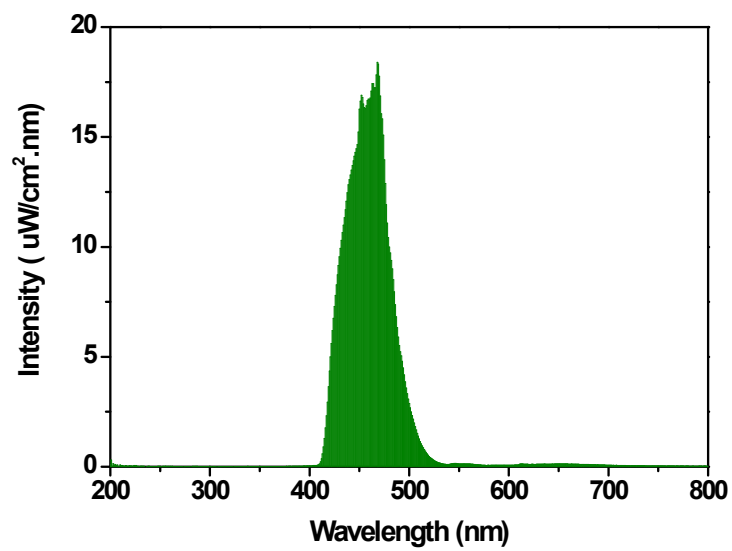


Figure S10. The light source for the visible light irradiation.

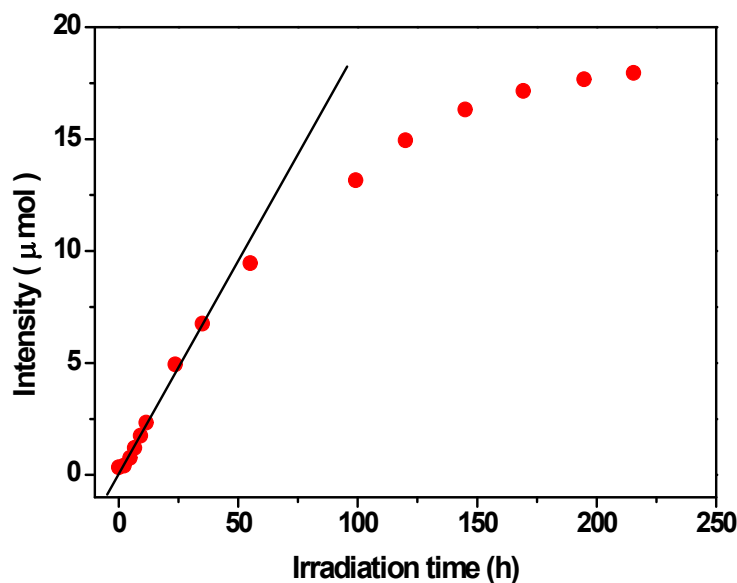


Figure S11. The CO₂ generation curve over Cu(II)-Nb_xTi_{1-x}O₂ (x=0.1 wt%) sample under visible light irradiation. The CO₂ generation rate (R_{CO_2}) was obtained from the slope of the CO₂ generation curve between the irradiation time of ca. 0 to 30 h.

The calculation of quantum efficiency (QE) was conducted using the same procedure reported in literature (*I*).

Take Cu(II)-Nb_xTi_{1-x}O₂ at x=0.1% sample for example. Under the visible light irradiation, the wavelength of visible light is from 400 to 530 nm, and the light intensity is 1 mW/cm². The irradiating area is 5.5 cm². Therefore, the absorption rate of incident photons (R_p^a) was determined to be 7.91×10^{14} quanta·sec⁻¹ using the following equation: $R_p^a = \int_{400}^{530} S \times \alpha \times I$ (S is the area of the sample, α is the light absorption and I is the light intensity at each wavelength). As for CO₂ generation, assuming that the reaction from IPA to CO₂ is proceeded: $C_3H_8O + 5H_2O + 18h^+ \rightarrow 3CO_2 + 18H^+$, that is, six photons are required to produce one CO₂ molecule. The CO₂ generation rate (R_{CO_2}) was obtained from the slope of the CO₂ generation curve in Figure S9. As shown in Figure S9, R_{CO_2} was determined to be 0.20 μmol·h⁻¹. Thus the QE for CO₂ generations were

calculated using the following equation:

$$\begin{aligned} \text{QE} &= 6 \times \text{CO}_2 \text{ generation rate} / \text{absorption rate of incident photon} \\ &= 6 \times (2.0 \times 10^{-1} \times 10^{-6} / 3.6 \times 10^3) \text{mol} \cdot \text{sec}^{-1} \times 6.0 \times 10^{23} \text{quanta} \cdot \text{mol}^{-1} \\ &\quad / 7.91 \times 10^{14} \text{quanta} \cdot \text{sec}^{-1} \\ &= 25.3 \times 10^{-1} (25.3\%). \end{aligned}$$

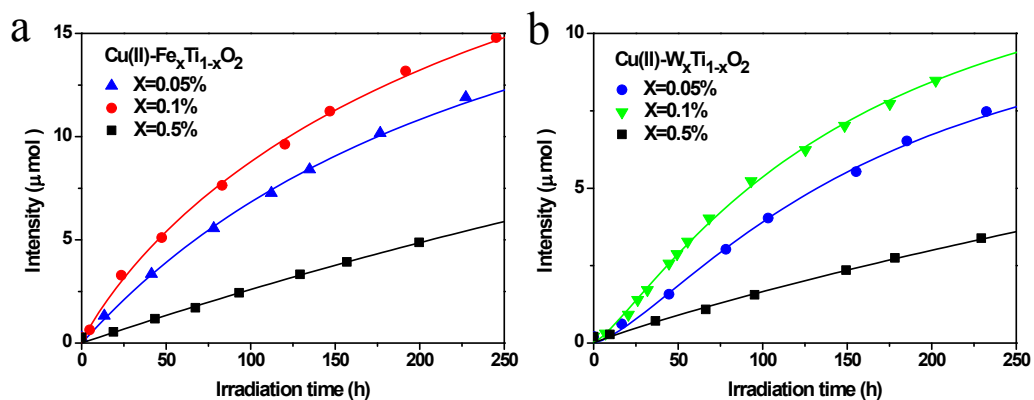


Figure S12. CO₂ generation over (a) Cu(II)-Fe_xTi_{1-x}O₂ at x=0.05 wt%, 0.1 wt%, and 0.5 wt%, and (b) Cu(II)-W_xTi_{1-x}O₂ at x=0.05 wt%, 0.1 wt%, and 0.5 wt%, under visible light irradiation.

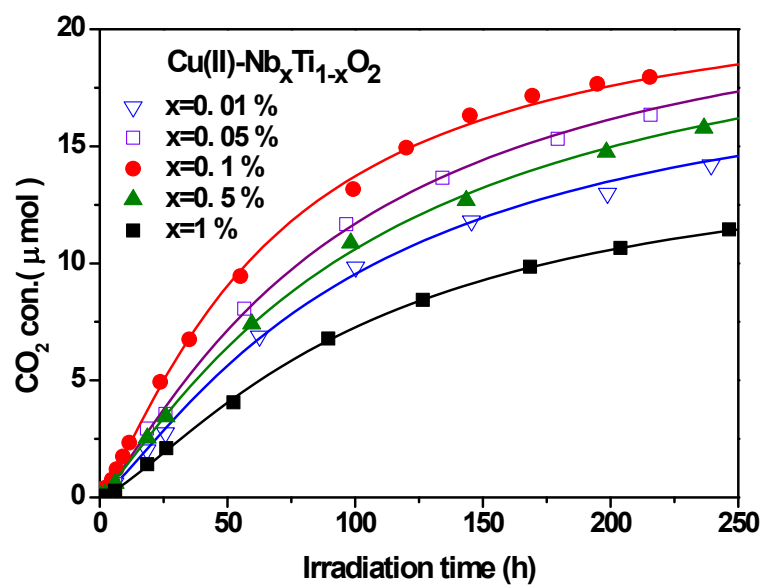


Figure S13. CO₂ generation over Cu(II)-Nb_xTi_{1-x}O₂ at x=0.01 wt%, 0.05 wt%, 0.1 wt%, 0.5 wt% and 0.5 wt% under visible light irradiation.

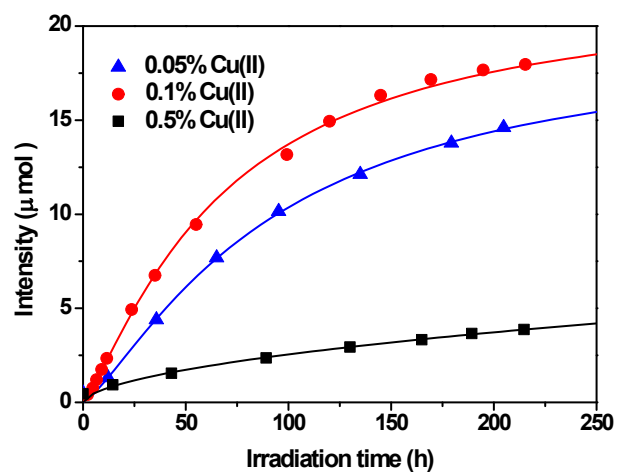


Figure S14. CO₂ generation over Cu(II)-Nb_xTi_{1-x}O₂ grafted with x=0.05 wt%, 0.1 wt%, and 0.5 wt% Cu(II) nanoclusters under visible light irradiation.

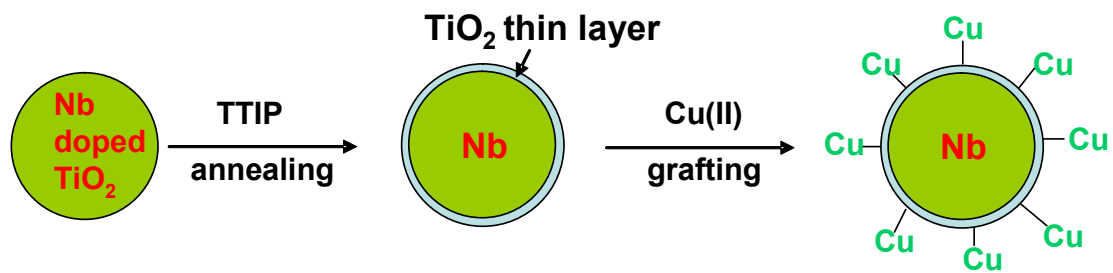


Figure S15. Scheme for the preparation of the samples by introducing a TiO₂ thin layer between Cu(II) nanoclusters and Nb_xTi_{1-x}O₂ (x=0.1 wt%).

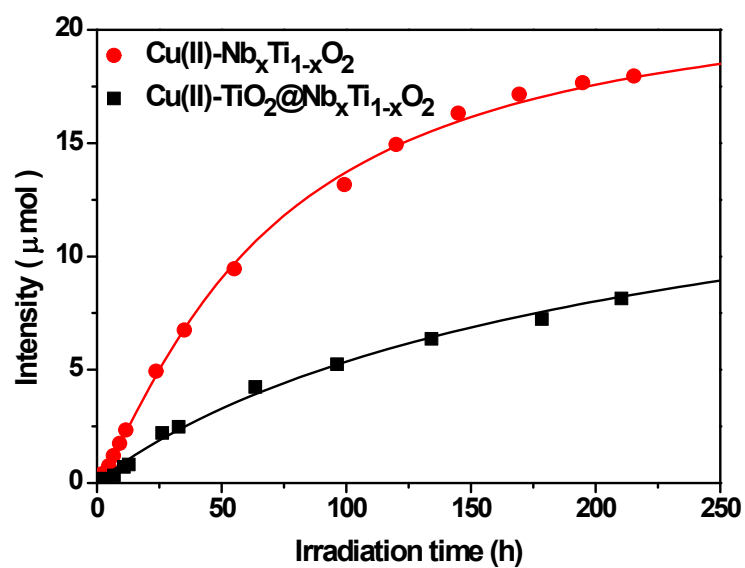


Figure S16. The CO₂ generation curve over Cu(II)-Nb_xTi_{1-x}O₂ and Cu(II)-TiO₂@Nb_xTi_{1-x}O₂ (x=0.1 wt%) samples under the same visible light irradiation.

References

1. H. G. Yu, H. Irie, Y. Shimodaira, Y. Hosogi, Y. Kuroda, M. Miyauchi, K. Hashimoto, *J. Phys. Chem. C* 2010, **114**, 16481-16487.